Revue des Sciences et Sciences de l'ingénieur
Journal of sciences and engineering sciences

ISSN 2170-0737 EISSN: 2600-7029

https://www.asjp.cerist.dz/en/PresentationRevue/303

Assessment of non-detection zone of different active anti-islanding methods for single and multi-inverters grid connected photovoltaic power systems

***Fadila Barkat[1], Ali Cheknane[1]**

1- Laboratoire des Semi-conducteurs et Matériaux Fonctionnels. Université de Laghouat, route de Ghardaïa, BP37G, Laghouat, Algérie

Article history
Received: 2018-03-29
Accepted: 2019-03-19
DOI: 10.34118/rssi.v8i1.1697

Abstract

This paper attempts to carry out a systematic study of the performance of the most common active detection methods, Active frequency drift (AFD) ,Sandia frequency shift (SFS) method and slip mode shift frequency (SMS) method. These methods are used to explain their global capability in developing photovoltaic system that are improved by including a boost converter MPPT technique and PID controller. Their effectiveness and limits in detection of islanding phenomenon are studied in details using Matlab/Simulink environment. In addition to that, the "no detection zone" of each method is basically investigated. The implementation of these methods shows that they can work perfectly under normal/islanded modes. Moreover, the results show that islanding mode can conditionally be detected and prevented successfully using the three common active methods when adequate parameters are adapted for the local load and for the grid. Moreover, the results show that there is an interaction between the used methods at the level of detection/prevention obtained in terms of time and non-detection zone.

Key-words: islanding; NDZ; active methods; inveters; PV

Résumé

Cet article tente de réaliser une étude systématique de la performance des méthodes de détection active les plus courantes, la méthode Active frequency drift (AFD) et Sandia frequency shift (SFS) et la méthode slip mode shift frequency (SMS). Ces méthodes sont utilisées pour expliquer leur capacité globale à développer des systèmes photovoltaïques améliorés en incluant une technique de convertisseur élévateur MPPT et un contrôleur PID. Leur efficacité et leurs limites dans la détection du phénomène d'îlotage sont étudiées en détail dans l'environnement Matlab / Simulink. En plus de cela, la «zone de non détection» de chaque méthode est fondamentalement étudiée. La mise en œuvre de ces méthodes montre qu'elles peuvent parfaitement fonctionner en mode normal / en îlot. De plus, les résultats montrent que le mode d'îlotage peut être conditionnellement détecté et empêché avec succès en utilisant les trois méthodes actives courantes lorsque des paramètres adéquats sont adaptés à la charge locale et au réseau. De plus, les résultats montrent qu'il existe une interaction entre les méthodes utilisées au niveau de la détection / prévention obtenu en termes de temps et de zone de non-détection

Mots-clés : Anti ilotage , , Islanding, Islanding-detection method, Active method, Simulation, Modeling, *Grid-connected, Photovoltaic, Inverter*

* Corresponding author. Tel. /fax: +213790139890.
E-mail address: f.barkat@lagh-univ.dz (Fadila Barkat).

1. Introduction

(PV) systems have become one of the most attractive power generation methods. The main purposes of utilizing distributed generator are assuring high power quality, highly efficient operation, and safety of the power system. However, an islanding condition may occur when a DG and the local loads are disconnected from the grid of DGs supplying power into the local loads. Unintentional islanding of a DG results in low power-quality, interference to grid-protection devices, equipment damage, and even personnel safety hazards. Therefore, islanding detection method (IDM) is needed and it has become a mandatory feature specified in the IEEE Std. 1547.1, IEEE Std. 929-2000, and UL1741 standards. IDMs are classified into passive and active methods. The passive methods use a trip function for an over/under voltage and frequency detection (UFP/OFP), phase jump detection, and voltage harmonic monitoring. Therefore, passive methods are costly and the accuracy of these methods is questionable. They also have a large non-detection zone (NDZ). In the meanwhile, active methods make a perturbation into the output current by injecting an active signal and monitor the change in the magnitude, frequency, or phase of the VPCC when an islanding condition occurs. Active methods use output power variations, active frequency drifts, and sliding mode frequency shifts. They can reduce the NDZ as compared to the passive method but degrade the power quality (current distortion) and the output power generated. These methods are not costly and they more recommended.

However, it is believed that if two or more solar inverters are connected to the same point of the common coupling point, their performance may degrade and can fail in detecting an islanding. Thus, it is necessary to analysis the non-detection zone of current islanding detection methods. In this paper the commonly used active methods namely active frequency drift (ADF), Sandia frequency Shift (SFS) and slip mode frequency shift (SMF) are comprehensively investigated for one and multiple inverter system in terms of non-detection zone.

2. Modeling of distribution generation system considering islanding requirements

In general, a PV based distributed generation unit is consisted of a PV array, DC/AC inverter, load (parallel RLC), switch (breaker or fuse). Islanding of a distributed generation unit, photovoltaic system for example, can occur when a part of the utility is disconnected from the main grid power supply, while it is still powered by the nearby distributed generation unit. Figures 1a and 1b show the developed models for the adapted PV system with normal operation and islanding modes.

In these figures, the RLC load is applied to represent the local load and the grid tied together at the PCC point. In the meanwhile, a breaker is placed to simulate the occurrence of the islanding. In general the active (P) and reactive (Q) power consumed by the RLC load are the sum of the inverter output power (Pinv and Qinv) and power from grid. However, in islanding condition, ΔQ and ΔP are assumed to equal zero [3]

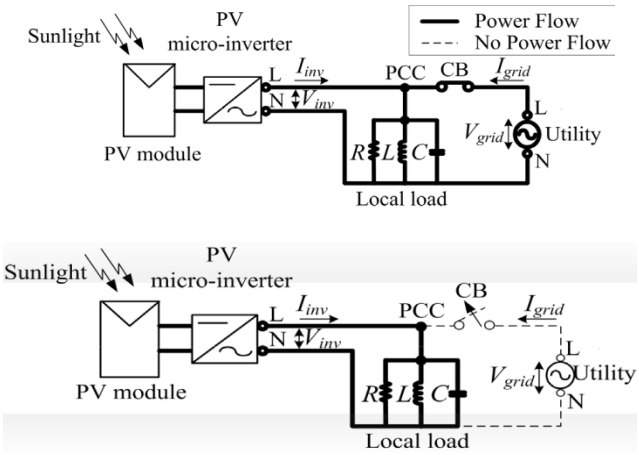

Fig. 1. Single PV micro-inverter system configuration without and with Islanding phenomenon mode

In this paper the distribution generation is considered to be in a unitary power factor operation. This unity power factor condition is combined with passive parameters of parallel RLC load and frequency. Moreover, the worst case for islanding detection is considered according to IEEE 929. The conditions of this case are described in detail below

- The power generated by DG should match the load power.
- The resonant frequency of the load is assumed as the same as grid line frequency.
- The quality factor (Qf) of the load is set to be 2.5. The quality factor is defined as that the reactive power stored in L or C times the active power consumed by R.

Under these conditions, when the grid is disconnected, the distributed generation and RLC load will resonate at nominal voltage and frequency to form an island. Otherwise there is a mechanism to drive voltage at PCC or frequency out of their nominal range. Load components and frequency can be descried as below

$$f = {}^{1}\!/_{2\pi\sqrt{LC}} \quad (1)$$

$$R = {}^{V^2}\!/_{P} \quad (2)$$

$$L = {}^{V^2}\!/_{2\pi f \mathrm{Q}_f P} \quad (3)$$

$$C = {}^{P\mathrm{Q}_f}\!/_{2\pi f \mathrm{Q}_f V} \quad (4)$$

Where R is effective load resistance (W), L is effective load inductance (H), C is effective load capacitance (F), P is active power (W), Qf is quality factor and f is grid frequency (Hz).

The values of frequency and voltage at the PCC after grid disconnection (islanding condition) depend heavily on the local load characteristic as illustrated in the relations below,

$$P_{load}={V_{PCC}^2}/{R} \quad (5)$$

$$Q_{load}= V_{PCC}^2\left(\frac{1}{WL}-wC\right) \quad (6)$$

i_{pv} and v_a must be ensured in in-phase as described in the equation below [2,3]

$$\arg[[R^{-1}+jwL^{-1}+jwC^{-1}]^{-1}]=0 \quad (7).$$

As mentioned previously, the power mismatch plane is inadequate to determine the non-detection zone of frequency drift active methods. This is because, for a fixed reactive power mismatch, more than one combination of L and C are possible [13]. However, by using the quality factor of the load as a parameter, the various combinations of RLC loads can be considered.

As mentioned previously, the quality factor is defined as the ratio of the stored energy to the dissipated energy per cycle at a given frequency. The quality factor for a parallel RLC load can be calculated as follows,

$$Qf \quad =\frac{2\pi\left(\frac{1}{2}CR^2I^2\right)}{\pi RI^2/w_0}=w_0RC=\frac{R}{w_0L}=R\sqrt{\frac{C}{L}} \quad (8)$$

Where w_0= (1 / *LC*) and it is the resonant frequency of the load.

The magnitude and the phase of a parallel RLC load in terms of the resonant frequency *f0* and arbitrary frequency are given as follows,

$$Z={1}/{\sqrt{\frac{1}{R}+\left(\frac{1}{wL}-wC\right)^2}}=\frac{R}{\sqrt{1+Q_f{}^2\left(\frac{f_0}{f}-\frac{f}{f_0}\right)^2}} \quad (9)$$

$$\emptyset_{load}=\tan^{-1}\left(R\left(\frac{1-w^2LC}{wL}\right)\right)=\tan^{-1}\left[Q_f\frac{f_0}{f}-\frac{f}{f_0}\right] \quad (10)$$

To determine the NDZ of active frequency drift methods, the phase angle of the current needs to be approximated. Sandia frequency shift (SFS), active frequency drift (AFD) and the frequency jump methods usually insert dead time into the current reference. As these methods are very similar to each other, only NDZ of SFS and AFD are determined. The NDZ of the slip mode frequency shift method is also determined, as it also drifts the frequency, but without the insertion of a dead time.

3. Islanding detection methods comparison

For a parallel RLC load, the load phase angle Q_(load) versus frequency characteristic curves of loads with different quality factors and different resonant frequencies f_0are shown in figure 2. In the meanwhile, the load current –voltage phase angle versus frequencies with different quality factor and different resonant frequency are shown in figure 3. It can be seen from these figures that for larger Q_f ,the resonant frequency of load have more effect on load output characteristics. The load impedance also varies under different frequency of an AC system. In meanwhile Figure 3 shows information of various kinds of load conditions; which may result different system performance.

3.1 Non-Detection Zone of The AFD Method

AFD method can be implemented either by adding a constant zero current segments or by forcing the current frequency to be always above or below the voltage frequency in the previous cycle. When the disconnection occurs, the frequency of the voltage at PCC tend to drift downward reaching a value that is higher than for [5]

For an AFD implemented with a constant frequency drift, the current in each cycle can be expressed by

$$I_k=\sqrt{2}I\sin\left[2\pi\left(\left(f_{v(k-1)}+\Delta f\right)\right)t\right] \quad (11)$$

Under islanding condition the inverter AFD angle can be approximated by, [5,6]:

$$\theta_{AFD}=\pi f t_z=\pi*\frac{\Delta f}{f+\Delta f} \quad (12)$$

This phase angle plays an important role in mapping the non-detection zone (NDZ) which be discussed after.

The AFD method uses two different chopping fractions every half-line cycle while the conventional one use single chopping fraction every whole line cycle. This means that the proposed chopping fraction can break the resonance at the frequency of the whole line cycle. Figure 4 shows the AFD reference current waveforms with two different chopping fractions; One is positive while the other is negative every half-line cycle. The AFD reference current wave form in Figure 4 can be defined as:

$$I_{AFD}(t)=\begin{Bmatrix} I\sin\left(2\pi f' t\right) & 0\le wt<\pi\text{-}t_z \\ 0 & \pi\text{-}t_z\le wt\le\pi \\ I\sin\left(2\pi f' t\right) & \pi\le wt<2\pi\text{-}t_z \\ 0 & 2\pi\text{-}t_z\le wt\le 2\pi \end{Bmatrix} \quad (13)$$

Where f is the frequency of the grid voltage, f' the frequency of the AFD current and which is express by

To calculate the NDZ, a combination between frequencies PCC voltage and load parameters is needed as illustrated in the equation below,

$$f_0^2-\frac{f_{is}\tan(\theta_{AFD}(f_{is}))}{Q_f}f_0-f_{is}^2=0 \quad (14)$$

$$f' = f\frac{1}{1-cf}$$

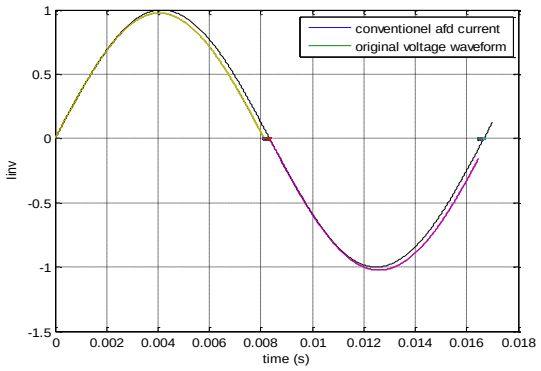

Fig. 2. Simulated waveform used by AFD

Based on that, the frequency is adjusted to the threshold frequency (fmin: 49Hz and fmax:51 Hz) by substituting f_{is} with (fmin ;fmax). Here NDZ can be represented in load parameter space as shown in Fig. 3

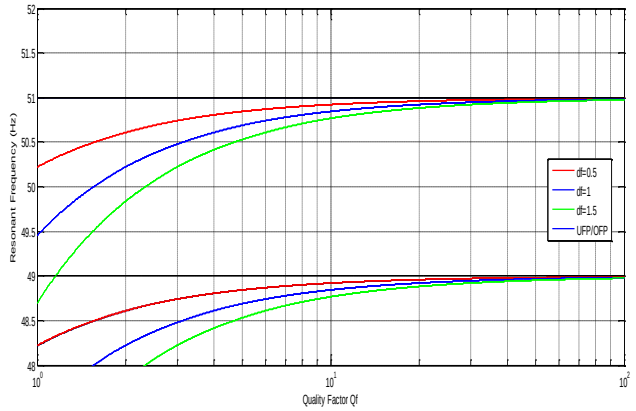

Fig. 3. NDZ of AFD islanding detection method

Fig. *5* shows the NDZ for AFD IDM for different values of df for a normal frequency range of 49H.z *≤f≤50.Hz.* from the figure it is clear that NDZ is shifted to lower values of f_o as Q increases. In the meanwhile, For Q_f=2.5 and df= 0.5 the method fails to detect islanding for loads with frequencies in the range of *48.69Hz≤f≤*50.69Hz. Moreover, If df is increased to 1Hz, islanding occurs for loads that have frequency in the range of 48.38*≤f≤50.38 Hz* .In both cases, the size of the range of resonant frequencies *(Δf=* f_{0max}- - f_{omin}) for which islanding occurs is the same as passive IDMs. Therefore, AFD does not yield a sizable reduction of NDZ as compared to the passive IDM (df= 0). Consequently, in low Q_f area and for higher frequency variation value in AFD, the system has less NDZ and can detect islanding more easily. When the quality factor of system load is high, the performance of AFD method is similar to the passive IDMs.

3.2 The Sandia Frequency Shift Method

The sandia frequency shift (SFS) IDM is based on the use of one zero current segment (tz) line semi cycle. A positive feedback is used to increase the chopping factor (cf) which is defined as the ratio of the zero time tz to half of the period of the voltage, thus,

$$Cf=\frac{2t_z}{T_u} \quad (15)$$

By increasing deviation of the frequency away from the nominal value, the increasing deviation is usually can be described by a linear function of the PCC voltage as below,

$$cf = cf_0 + k(f - f_g) \quad (16)$$

$$\theta_{SFS} = \frac{\pi}{2}(cf_0 + k\Delta f) = 2\pi f\frac{t_z}{2} \quad (17)$$

here cf_0 is the chopping fraction and k is an gain .for a cf_0=0.03 and $\Delta f = 1Hz$

The NDZ of the SFS in the Q_F versus f_0 is derived using the phase criteria is illustrated below,

$$\tan^{-1}\left[Q_f\left(\frac{f_0}{f_{is}} - \frac{f_{is}}{f_0}\right)\right] = \frac{\pi}{2}\left[cf_0 + k(f_{is} - f_g)\right] \quad (18)$$

Fig. 4 shows NDZ of a solar inverter equipped with SFS. From the figure, the NDZ is null for loads with $Q_f \leq 4.8$ when cf_0=0.03 and k=0.1. Besides, as k decreases the SFS method performance becomes similar to AFD. Therefore, the performance of this method is quite similar to the passive IDM in case of loads with high Q_f

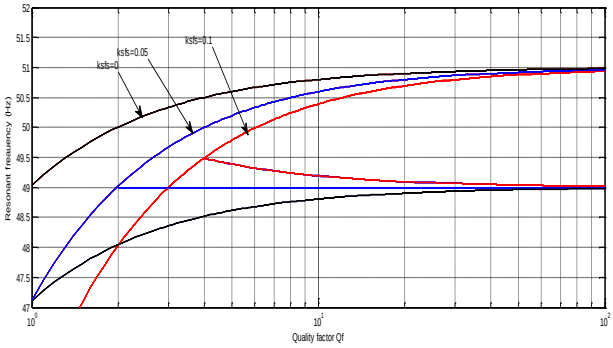

Fig. 4. NDZ of SFS method

3.3 The slip mode frequency shift

The slip mode frequency shift (SMS) changes the phase angle of the solar inverter current θ_(SMS) according to the variation of the measured voltage frequency with respect to the nominal frequency of the electrical grid as illustrated below, Where f_m is the

frequency when θ_m arise and $f_m - f_0$ is assumed to equal to 3 Hz. AS Figure 5

In order to cover islanding considering typical characteristic of a solar inverter such as the one presented in [3], the biggest slope of Eq. (23) for the interval of 49–50Hz is chosen as the slope of the straight characteristic line. The advantage of Eq. (23) is obvious: it allows for an easier implementation as compared to the original sinusoidal representation of the phase angle–frequency relation (see fig. 7)

$$\theta_{sms.k} = \frac{2\pi}{360}\theta_m \sin\left(\frac{\pi}{2}\frac{f-f_0}{f_m-f_0}\right) \quad (19)$$

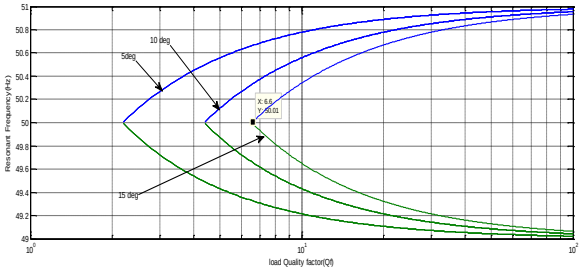

Fig. 5. NDZ of SMS anti islanding method

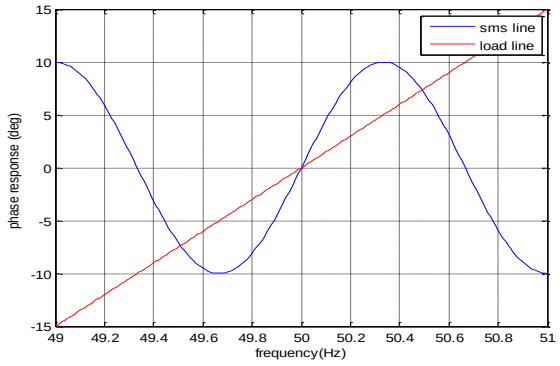

Fig. 6. Frequency phase curve of load line and SMS line

In general, the utility stabilizes the operating point at the line frequency by providing a solid phase and Frequency reference while it is connected. However, after grid disconnection, the phase-frequency operating point of the load and solar inverter must meet at an intersection point of the load line and the inverter phase response curve as follows,

$$\frac{d\theta_{load}}{df} = \frac{d\theta_{sms}}{df} \quad (20)$$

Fig 6 shows the SMS and the load phase response curves with stable and unstable intersection points. The main parameters of the SMS system (θ_m and f_m) should be designed so that there are no stable intersection points within the normal operating range of the over/under frequency devices, otherwise it would not trip under islanding conditions, This condition is met when,

$$\left.\frac{d\theta_{load}}{df}\right|_{f=fg} \leq \left.\frac{d\theta_{sms}}{df}\right|_{f=fg} \quad (21)$$

By using calculations and simplifications reported in [11-12] it is found that,

$$\theta_m \geq \frac{12Q_f}{\pi^2}(f_m - f_g) \quad (22)$$

θ_m can be chosen according to the load factor at which the islanding is expected to be detected by SMS. Based on IEEE std. 929-2000, the worst case happens when load Q_f=2.5, and the resonant frequency are close to the grid frequency. Thus, the SMS system is designed for a worst case load condition (Q_f =2.5 or above). This to say that this method may fail to detect islanding for cases with Q_f lower than 2.5.

The NDZ of SMS in the Q_f versus f_0 space can be derived using the phase criteria

$$tan^{-1}\left[Q_f\left(\frac{f_0}{f_{is}} - \frac{f_{is}}{f_0}\right)\right] = \theta_m \sin\left(\frac{\pi}{2}\frac{f_{is}-f_g}{f_m-fg}\right) \quad (23)$$

The resulting NDZ for SMS in the Q_f versus f_0 space is obtained from the solution of equation 27 and shown in figure 8($\theta_m = 10°$ and fm-fg=3Hz). From the figure, as θ_m decreases, the load quality factor for which islanding occurs also decreases. Here also the performance of this method is similar to the passive over/under frequency based methods. ($\theta_m = 0°$) for loads with high Q_f.

4. NDZ for PV systems with tow solar inverters

In order to compare the performance of the evaluated active anti islanding methods and the effect of interaction in case of two solar inverters connected to the same PV grid connected system, the size of the NDZ has been evaluated for different system topologies. Figure 7 shows the modeled systems with two solar inverters.

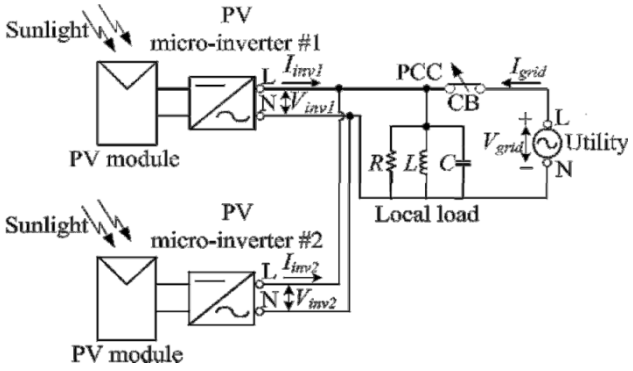

Fig. 7. Two PV micro-inverter systems for islanding detection test

4.1 Case I One inverter is equipped with AFD and SMS Methods

In this section perturbation interference and detection performance in two inverters will be simulated and analyzed. In this case the AFD and SMS will be considered. Assume that there are two inverter's current can be described as below,

$$i_{AFD} = \sqrt{2}k_{AFD} I \sin(2\pi f t + \theta_{AFD}) \quad (24)$$

$$i_{SMS} = \sqrt{2}k_{sms} I sin(2\pi f t + \theta_{sms}) \quad (25)$$

Where k_{AFD} is the proportional of active power provided by the inverter equipped with AFD IDM, and k_{SMS} is the same at the SMS case

θ_{AFD} is the initial phase of the inverter equipped with the AFD method and thus,

$$\theta_{AFD} = \frac{(2\pi f)t_z}{2} = \pi \frac{\Delta f}{f+\Delta f} \quad (26)$$

Where, t_z is dead time area, f is the last period frequency inverter output voltage, Δf is frequency shifting of inverter output voltage,

$$\theta_{SMS} = \theta_m \sin\left(\frac{\pi}{2}\frac{f-f_g}{f_m-f_g}\right) \quad (27)$$

According to the later formula, the two inverters can be considered equivalent to one inverter [5]. The equivalent inverter output current can be then described as below,

$$\theta_{inv} = \tan^{-1}\left(\frac{k_D \sin\theta_{AFD} + (1-K_D)\sin\theta_{SMS}}{K_D \cos\theta_{AFD} + (1-K_D)\cos\theta_{SMS}}\right) \quad (28)$$

Thus the $Q_f \times f_0$ frame is determined by:

$$f_{is}^2 + \frac{f_0 \tan(\theta_{INV}(f))}{Q_f} f - f_0^2 = 0 \quad (29)$$

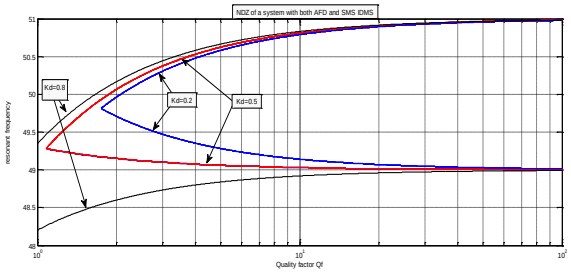

Fig. 8. NDZ of a system with both AFD and SMS IDMs

Fig. 8shows NDZ for PV system with both AFD and SMS IDMs (Δf is 1Hz,θ_m is $10°$ and (f_m-f_g) is $3Hz$)

4.2 Case III: Both inverters are equipped with both SFS IDMs

In general, there is a measuring error when sensors measure the frequency of voltage, so the frequency measured in the two inverters is supposed to be $f_1 = f + \Delta f$ and $f_2 = f - \Delta f$ respectively. When using the SFS method, if the actual frequency f is more than reference the frequency f_0, f will either rise or drop. Therefore, the system operating frequency of these two inverters changes reversely because of the sensors measuring error. Thus, the islanding detection function of the two inverters disturbs mutually (the so-called dilution effect), and the probability of islanding occurrence is enlarged [9].

In order to have a convenient analysis, the initial chopping cf_0 and positive-feedback gain k of the two inverters are supposed to be the same. First, the two inverters are equivalent to one inverter, the output current of equivalent inverter is,

$$i_{INV} = \sqrt{2}\frac{I}{2}[\sin(2\pi f_1 t + \theta_{SFS1}) + \sin(2\pi f_2 t + \theta_{SFS2})] \quad (30)$$

If the value of Δf is small enough, we can obtain the approximate expression

$$i_{INV} \approx \sqrt{2}I\cos\left(\frac{\theta_{SFS1}-\theta_{SFS2}}{2}\right)\sin\left(2\pi ft + \frac{\theta_{SFS1}+\theta_{SFS2}}{2}\right) \quad (32)$$

$$\approx \sqrt{2}I_{INV}\sin(2\pi f t + \theta_{INV}) \quad (33)$$

Where

$$\theta_{INV} = \frac{\theta_{SFS1}+\theta_{SFS2}}{2} = \frac{\pi}{2}(cf_0 + k\Delta f) \quad (34)$$

Fact because of the frequency measuring error, the positive-feedback perturbations are produced by the two inverters counteract mutually. However, the initial chopping and positive-feedback gain still exist. In the meanwhile, the frequency positive-feedback can be still triggered without affecting the islanding process. Therefore, the NDZ for

From the figure the NDZ is enlarged along with the augment of Kd which proportion of local load's active power provided by the inverter equipped with AFD IDM [5].

4.3 Case II: two Inverters are equipped with AFD and SFS IDM

In this part two inverters are equipped one with AFD and other with SFS therefore the two inverters currents can be expressed as still assumed that the frequency of the two inverters has a sensor measuring error, and the error is +Δf and –Δf respectively. This is to say, the error amplitude is the same and the error polarity is the opposite. Then the output current of equivalent inverter is

$$i_{AFD} = \sqrt{2}K_{AFD}Isin(2\pi ft + \theta_{AFD}) \quad (35)$$

$$i_{SFS} = \sqrt{2}(1 - K_{AFD})I\sin(2\pi ft + \theta_{SFS}) \quad (36)$$

$$i_{INV} = \sqrt{2}\frac{I}{2}[\sin(2\pi f_1 t + \theta_{SMS}) + \sin(2\pi f_2 t + \theta_{SMS})] \quad (37)$$

By assuming the value of Δfe small enough, then the approximate expression below can be used,

$$i_{INV} \approx \sqrt{2}Icos\left(\frac{\theta_{sms1} - \theta_{sms2}}{2}\right)\sin\left(2\pi ft + \frac{\theta_{sms1} + \theta_{sms2}}{2}\right) \quad (38)$$

$$\approx \sqrt{2}I_{INV}\sin(2\pi ft + \theta_{INV} \quad (39)$$

Where

$$\theta_{inv} = \theta_{meq}\sin\left(\frac{\pi}{2}\frac{f - f_g}{f_m - f_g}\right) \quad (40)$$

$$\theta_{meq} = \theta_m\cos(\frac{\pi}{2}\frac{\Delta f}{f_m - f_g}) \quad (41)$$

With this method, the frequency measuring error will reduce the amplitude of maximum phase shifting angle θ_m, it means that the positive-feedback perturbations produced by the two inverters counteract mutually, and the NDZ will increase, so the performance of islanding detection will drop. However, even if the measuring error Δf takes a relatively big value (0.5 Hz), and fm – fg=3Hz, the maximum phase shifting angle θmeq drops only 3.4% compared with [9]. In addition, there is not an obvious change for the NDZ. Figure 9 shows the NDZ for different Δfe (θm = 10°、fm – fg =3Hz). This figure indicates that though the frequency measuring error makes the perturbation produced by the two inverters counteract mutually, it almost has no impact on the performance of islanding detection [9].

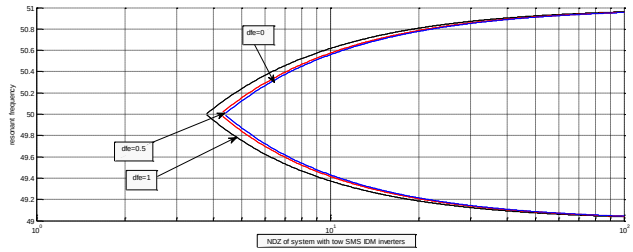

Fig. 9. Figure 13 NDZ of a system with both SMS IDM inverters

5. Testing system development

Figure 10 shows the block diagram of the system used in this study. It consists of a PV block, DC-DC boost converter that is controlled by MPPT technique, an inverter that is controlled by hysteresis block, an injecting block for currents of anti-islanding method, a block that measures the voltage and frequency and a block that produces fault signal based on the UOF/UOV passive method.

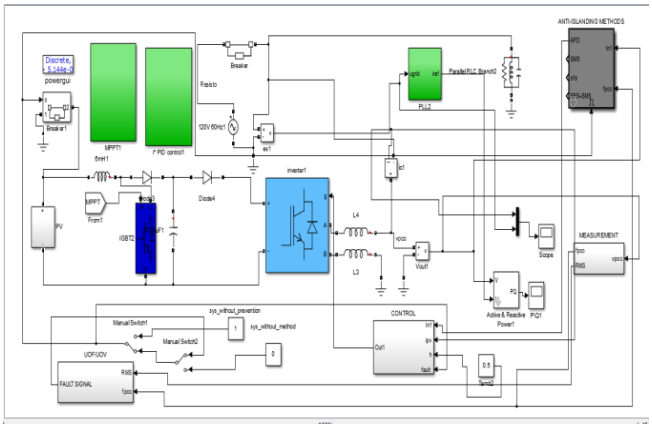

Fig. 10. Simulink model of the testing system

The parameters of the system that is connected to a 120V, 60Hz single phase low voltage distribution system are listed in Table 1.

Table 1. Islanding testing condition for developed system according to IEEE std.929

Parameter	Value
Nominal line frequency (f0) [Hz]	60
Grid voltage (Vg)[V]	250
Resistance (R)[Ω]	14.4
Inductance (L)[mH]	15.28
Capacitance (C) [μF]	460.5
DG output power [kW]	1
INPUT DC voltage [V]	250
F (min/max)[Hz]	59.3/60.5
Q_f	2.5

5.1 AFD method results

Figures 11 a and b show the time domain response of the system with AFD method in terms of voltage V, current IPV, fault signal and the frequency with df = 1Hz. From the Figures, it can be seen that with the present value of reference current, the magnitude of the voltage does not have apparent change before and after the disconnection of the grid for a certain time.

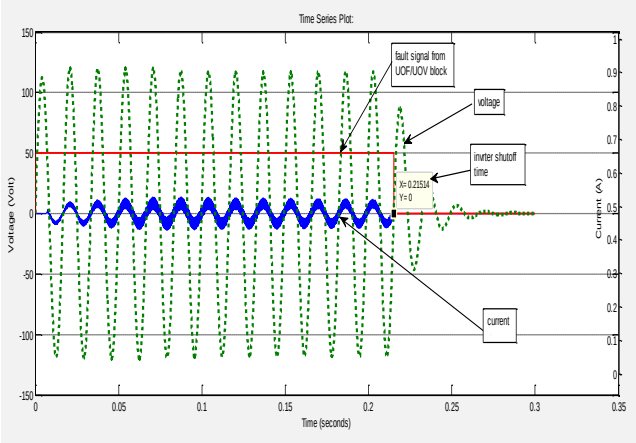

(a)

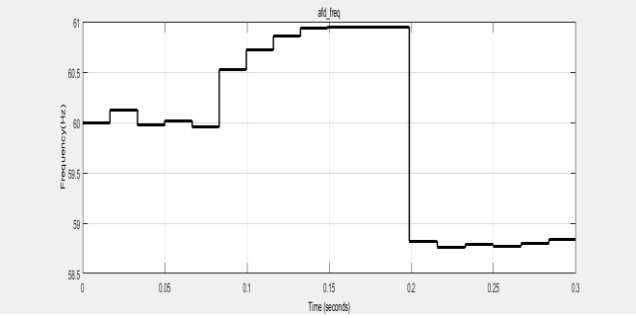

(b)

Fig. 11 Islanding detection test for an inverter with SFS IDM:K_{SFS}=0.018Hz^{-1},PCC voltage, inverter current; and fault signal wave forms. (a) Voltage frequency values

5.2 SFS method results

Figures 12 show the implementation of voltage and currents in the time domain and the frequency f using SFS method for value of Ksfs 0.018 Hz^{-1}The critical detection time was t=0.18157s^{-1} noting that with Ksfs=0Hz^{-1}, SFS method became similar to the AFD method. After the islanding frequency detection point, the generator lost its stability when Ksfs=0.018Hz^{-1}, while the islanding is detected in a short time. However, the island frequency reached 60.5 Hz in a long time

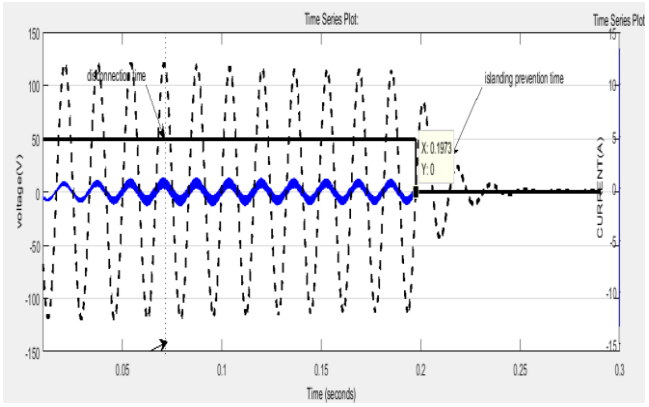

(a)

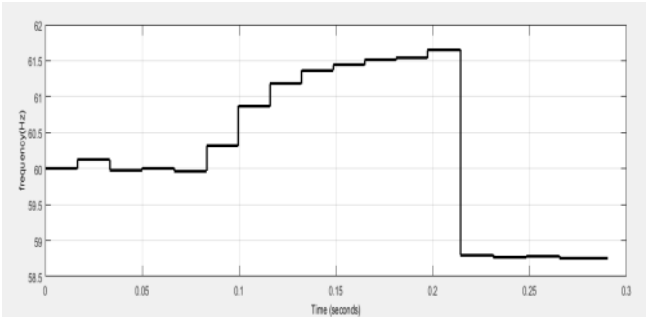

(b)

Fig. 12. Islanding detection test for an inverter with SFS IDM:K_{SFS}=0.018Hz^{-1},PCC voltage, inverter current; and fault signal wave forms. (a) Voltage frequency values

5.3 . SMS method results

Similar tests were done for the grid connected inverter using the SMS AIM with different values for θm(15°). Figs. 13 show the time domains response of the system with SMS AIM in terms of voltage VPCC, current IPV, fault signal, the frequency fPCC in each condition (θm values)

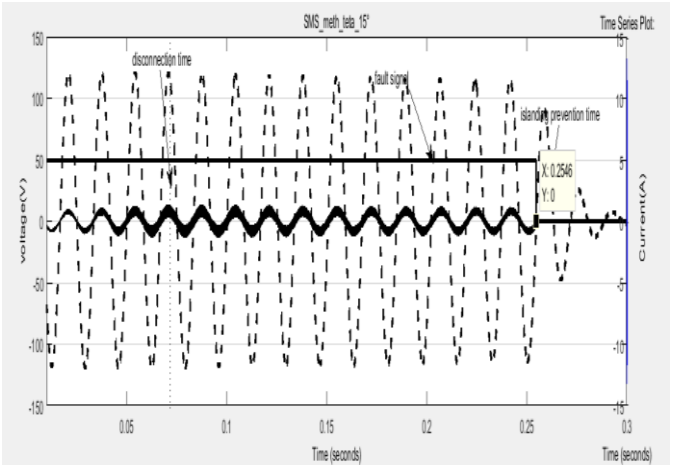

(a)

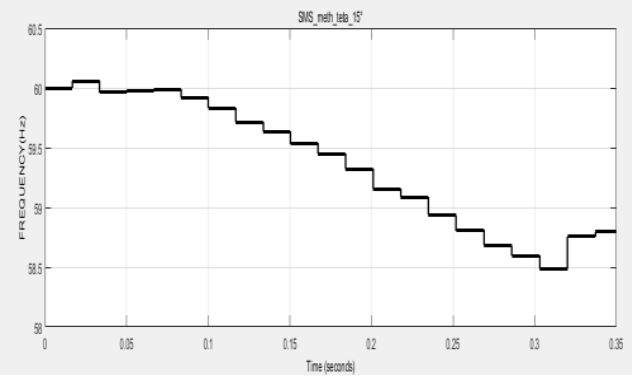

(b)

Fig. 13 Islanding detection test for an inverter with SMS IDM:teta=15^0 PCC voltage, inverter current; and fault signal wave forms. (a) Voltage frequency values

6. Conclusion

This paper discussed three active islanding techniques namely AFD SMS and SFS. The adapted testing system consisted of a PV system with a boost converter that was controlled by MPPT and PID controller. The over/under voltage and frequency protection methods were also identified as default protection methods as they are adaptable with the suggested system and easy to implement.. The non-detection zone for each method was basically discussed for different cases based on the mathematical consideration . The simulation results of this study have been utilized to compare between the selected methods in order to verify their effectiveness, and compatibility with testing system. The results showed that the conducted simulation confirmed the effectiveness of the investigated methods on the suggested grid connected system under varying parameters for local load and frequency.

References

[1] Bhandari, R., Gonzalez, S., &Ropp, M. E. (2008, July). Investigation of two anti-islanding methods in the multi-inverter case. In Power and Energy Society General Meeting-Conversion and Delivery of Electrical Energy in the 21st Century, 2008 IEEE (pp. 1-7). IEEE.

[2] Xu, M., Melnik, R. V., &Borup, U. (2004).Modeling anti-islanding protection devices for photovoltaic systems. Renewable Energy, 29(15), 2195-2216.

[3] Li, X., &Balog, R. S. (2014, August).Analysis and comparison of two active anti-islanding detection methods. In Circuits and Systems (MWSCAS), 2014 IEEE 57th International Midwest Symposium on (pp. 443-446). IEEE.

[4] ROPP, M. E., BEGOVIC, Miroslav, et ROHATGI, A. Analysis and performance assessment of the active frequency drift method of islanding prevention. Energy Conversion, IEEE Transactions on, 1999, vol. 14, no 3, p. 810-816.

[5] ZHANG, Xing et XIE, Dong. Performance Assessment of Islanding Detection for Multi-inverter Grid-connected Photovoltaic Systems. Energy and Power Engineering, 2013, vol. 5, no 04, p. 1517.

[6] Estébanez, E. J., Moreno, V. M., Pigazo, A., &Liserre, M. (2011). Performance evaluation of active islanding-detection algorithms in distributed-generation photovoltaic systems: Two inverters case. Industrial Electronics, IEEE Transactions on, 58(4), 1185-1193.

[7] Yu, B. (2014). An improved active frequency drift anti-islanding method for multiple PVmicro-inverter systems. IEICE Electronics Express, 11(6), 20140143-20140143.

[8] Yu, B., Matsui, M., & Yu, G , A review of current anti-islanding methods for photovoltaic power system. Solar Energy, 84(5), 745-754 (2010)

[9] Hong, Y., & Huang, W. (2014, November).Investigation of Frequency drifts methods of Islanding Detection with multiple PV inverters. In Electronics and Application Conference and Exposition (PEAC), 2014 International (pp. 429-434). IEEE.

[10] Wang, X., Freitas, W., &Xu, W. (2011). Dynamic non-detection zones of positive feedback anti-islanding methods for inverter-based distributed generators. Power Delivery, IEEE Transactions on, 26(2), 1145-1155.

[11] Lopes, L. A., & Sun, H. (2006).Performance assessment of active frequency drifting islanding detection methods. Energy Conversion, IEEE Transactions on, 21(1), 171-180.

[12] Yu, B., Matsui, M., Jung, Y., & Yu, G. (2007). Modeling and design of phase shift anti-islanding method using non-detection zone. Solar Energy, 81(11), 1333-1339.

[13] IEEE Recommended Practice for Utility Interface of Photovoltaic (PV) Systems, IEEE Std. 929-2000